Kinesin-dependent mechanism for controlling triglyceride secretion from the liver

Priyanka Rai[a], Mukesh Kumar[a], Geetika Sharma[b], Pradeep Barak[a], Saumitra Das[b], Siddhesh S. Kamat[c,d], and Roop Mallik[a,1]

[a]Department of Biological Sciences, Tata Institute of Fundamental Research, Mumbai 400005, India; [b]Department of Microbiology and Cell Biology, Indian Institute of Science, Bangalore 560012, India; [c]Department of Biology, Indian Institute of Science Education and Research, Pune 411008, India; and [d]Department of Chemistry, Indian Institute of Science Education and Research, Pune 411008, India

Edited by David W. Russell, University of Texas Southwestern Medical Center, Dallas, TX, and approved October 31, 2017 (received for review August 1, 2017)

Despite massive fluctuations in its internal triglyceride content, the liver secretes triglyceride under tight homeostatic control. This buffering function is most visible after fasting, when liver triglyceride increases manyfold but circulating serum triglyceride barely fluctuates. How the liver controls triglyceride secretion is unknown, but is fundamentally important for lipid and energy homeostasis in animals. Here we find an unexpected cellular and molecular mechanism behind such control. We show that kinesin motors are recruited to triglyceride-rich lipid droplets (LDs) in the liver by the GTPase ARF1, which is a key activator of lipolysis. This recruitment is activated by an insulin-dependent pathway and therefore responds to fed/fasted states of the animal. In fed state, ARF1 and kinesin appear on LDs, consequently transporting LDs to the periphery of hepatocytes where the smooth endoplasmic reticulum (sER) is present. Because the lipases that catabolize LDs in hepatocytes reside on the sER, LDs can now be catabolized efficiently to provide triglyceride for lipoprotein assembly and secretion from the sER. Upon fasting, insulin is lowered to remove ARF1 and kinesin from LDs, thus down-regulating LD transport and sER–LD contacts. This tempers triglyceride availabiity for very low density lipoprotein assembly and allows homeostatic control of serum triglyceride in a fasted state. We further show that kinesin knockdown inhibits hepatitis-C virus replication in hepatocytes, likely because translated viral proteins are unable to transfer from the ER to LDs.

lipid droplet | kinesin | ARF1 | VLDL secretion | hepatitis C

Cytosolic lipid droplets (LDs) are the primary cellular stores for triglyceride (TG), cholesterol, and sphingolipids (1). LDs interact physically with the endoplasmic reticulum (ER) to exchange lipids and proteins (2, 3). Such interactions appear key for the storage and catabolism of TG (4, 5), their aberrance leading to fatty liver (6). However, how LD–ER interactions are controlled by metabolic signals in an animal, and the resultant lipid fluxes are unknown because most studies use cultured cells (3, 5, 7–9). Here we address how ER–LD interactions are controlled across fed/fasted states in the liver of rats and how this helps establish systemic lipid homeostasis in the animal. TG is secreted as very low density lipoprotein (VLDL) particles from hepatocytes in the liver. Most (~70%) of TG in VLDL is derived from cytosolic LDs (10, 11). The liver stores ~100-fold less TG than adipose tissue, yet remarkably, both tissues secrete TG/fatty acids (FAs) at comparable rates. This happens because the release rate/steady-state mass of TG is 80-fold higher for liver compared with adipose tissue (12). In other words, a small pool of LDs in hepatocytes is efficiently and rapidly catabolized to supply TG for lipidating VLDL particles (10, 12). However, this situation changes dramatically after fasting, when adipose-derived fatty acid reaches the liver and is esterified into TG in hepatocytes leading to massive accumulation of LD TG in the liver (~4-fold increase; fasting induced steatosis). By sequestering away TG in this manner, the liver protects other organs from lipotoxic fatty acids (6, 13–15).

The existing literature on liver function puzzled us and posed a question which we believe has never been raised. If the efficient mobilization of LD TG continues uncontrolled from the substantially higher LD-TG pool in fasted liver, this would elevate circulating serum TG to dangerous levels after fasting. In reality, serum TG is almost unchanged across feeding–fasting cyles (13). We therefore wondered whether a (unknown) mechanism is activated to limit TG mobilization from LDs in the liver after fasting. We show here that such a mechanism indeed exists, and that it surprisingly involves kinesin-driven transport of LDs along microtubules (MTs) in hepatocytes. We find that kinesin-1 is recruited to LDs by the GTPase ADP ribosylation factor 1 (ARF1), a key activator of lipolysis on LDs (3). ARF1 and kinesin recruitment to LDs occurs downstream of an insulin-dependent pathway, and therefore both proteins appear abundantly on LDs in the liver in a fed state (insulin signaling high). Kinesin transports LDs to the periphery of hepatocytes inside liver, where the smooth ER (sER) is located, facilitating physical interactions between LDs and the sER. The major lipase that channels LD TG toward VLDL assembly is localized in the sER in hepatocytes (16), and VLDL assembly takes place in the sER (13). LD–sER interactions driven by kinesin in a fed state therefore facilitate efficient supply of TG from LDs toward assembly of VLDL particles. Most interestingly, fasting (lowered insulin signaling) reduces ARF1 and kinesin-1 on LDs to limit sER–LD interactions, thereby tempering supply of TG toward VLDL production and homeostatically controlling serum TG in the animal.

Lastly, our data suggest that in the absence of kinesin-1, freshly translated HCV proteins cannot transfer from the ER to LDs, a step that is essential for HCV replication (17). Taken together, we

Significance

The liver secretes lipids in a controlled manner despite vast changes in its internal lipid content. This buffering function of the liver is essential for lipid/energy homeostasis, but its molecular and cellular mechanism is unknown. We show that motor protein kinesin transports lipid droplets (LDs) to the endoplasmic reticulum (ER) in liver cells, engineering ER–droplet contacts and supplying lipids to the ER for secretion as lipoprotein. However, when fasting induces massive lipid accumulation in liver, kinesin is removed from LDs, inhibiting lipid supply to the ER and homeostatically tempering lipid secretion from liver in a fasted state. Interestingly, reducing kinesin also blocks propagation of hepatitis-C virus inside liver cells, possibly because viral proteins cannot transfer from the ER to LDs.

Author contributions: P.R., S.D., S.S.K., and R.M. designed research; P.R., M.K., G.S., P.B., S.S.K., and R.M. performed research; M.K., G.S., S.D., S.S.K., and R.M. contributed new reagents/analytic tools; P.R., M.K., G.S., P.B., S.S.K., and R.M. analyzed data; and P.R. and R.M. wrote the paper.

The authors declare no conflict of interest.

This article is a PNAS Direct Submission.

[1]To whom correspondence should be addressed. Email: roop@tifr.res.in.

This article contains supporting information online at www.pnas.org/lookup/suppl/doi:10.1073/pnas.1713292114/-/DCSupplemental.

elucidate a cellular and molecular mechanism that controls ER–LD interactions in the liver across metabolic states. This allows the liver to protectively sequester away massive amounts of lipotoxic TG in the form of benign LDs after fasting, and thus facilitates homeostatic and systemic control of circulating serum TG in the animal. HCV appears to take advantage of kinesin-induced ER–LD interactions to propagate its life cycle.

Results

Feeding–Fasting-Dependent Accumulation of LDs in the Liver. Massive increase in LDs was seen in rat liver after 16-h fasting, as also reported elsewhere (13, 14). This was clear from immunofluorescent staining of liver sections against the LD marker perilipin-2 (Fig. 1*A*), and also by TLC of liver tissue (Fig. 1*B*). Despite this accumulation of TG in liver, there was no change of TG in serum prepared from animals (Fig. 1*B*). Microsomes prepared from fed and fasted liver showed no difference in TG content (*SI Appendix*, Fig. S1*A*), suggesting that cytosolic LDs are the major site of TG accumulation in liver in a fasted state. These microsomes were enriched in ER components (*SI Appendix*, Fig. S1*B*). Magnified images of perilipin-2–stained LDs in liver sections from fed and fasted rats are shown in *SI Appendix*, Fig. S1*C*. The fasted liver had a larger number of LDs, but careful analysis revealed no change in the size of individual LDs after fasting (average diameter ~1.8 μm; *SI Appendix*, Fig. S1*C*). There was some variation (~20%) in TG staining in different parts of the liver from fed rats, possibly due to hypoxia. However, these differences were very small compared with the severalfold increase of TG staining seen in all parts of the liver after fasting.

To better understand their morphology, function, and lipid/protein content we next purified LDs from rat liver (18, 19). LDs purified from liver of normally fed and 16-h fasted rats will be denoted, respectively, as normal LDs (NLDs), and fasted LDs (FLDs). NLDs and FLDs were highly refractile and spherical organelles, again of similar size (*SI Appendix*, Fig. S1*D*). Immunofluorescence staining against perilipin-2 confirmed these organelles as LDs with largely intact membrane (*SI Appendix*, Fig. S1*E*). Individual NLDs and FLDs showed no difference in perilipin-2 amounts, as evidenced by equal intensity of staining (*SI Appendix*, Fig. S1*E*). The purified LD fraction was enriched in perilipin-2, with no detectable contamination from other organelles (*SI Appendix*, Fig. S2*A*). Clean separation of NLDs and FLDs into the most buoyant fraction suggests that they are TG rich (18, 19).

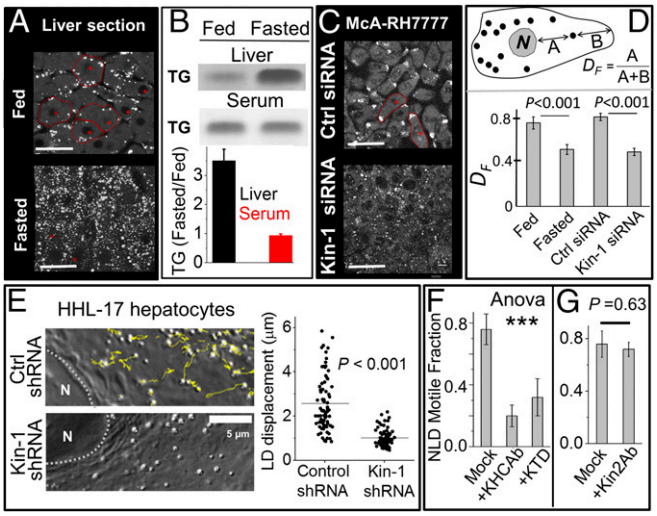

Fig. 1. Fasting-induced accumulation and kinesin-1–driven motion of lipid droplets. (*A*) Confocal image of liver sections from fed and fasted rats stained for perilipin-2. Experiments were done in four biological replicates. (Scale bar, 25 μm.) (*B*) TLC of crude liver extract (*Upper*) and serum (*Lower*) prepared from fed and fasted rats. Samples normalized to total protein. Each experiment was repeated three times. The relative changes (normalized to fed) are quantified. Error bars show SEM. (*C*) McA-RH7777 cells treated with control siRNA and siRNA against rat kinesin-1 were stained with BODIPY to label LDs. Some cells are outlined in red. (Scale bar, 25 μm.) (*D*) The fractional distance D_F of LDs from nucleus in liver section and McA-RH7777 cells (see figure for definition of D_F). Fifty LDs from at least 20 cells were used for each condition. Experiments were done in three biological replicates. Error bars are SEM. (*E*) Yellow lines show tracks for LD motion in a 20-s window in HHL-17 hepatocytes treated with control shRNA and shRNA against human kinesin-1. *Right* shows length of tracks. Horizontal lines denote mean. The Kolmogorov–Smirnov test was used to ascertain statistical significance. More than 70 LDs from 10 cells were used for each condition. Experiments were done in three biological replicates. (*F*) Motile fraction of NLDs after incubation with KHC Ab (kinesin-1 antibody) and KTD (kinesin tail domain) peptide. Experiments were done in three biological replicates. Error bars are SEM. One-way ANOVA showed that means of the three conditions were not equal [$F(2, 6) = 49.56$, $^{***}P < 0.001$]. A Tukey post hoc test showed difference between "mock" and the two other groups (KHCAb and KTD). No difference was seen between KHCAb and KTD. (*G*) Motile fraction of NLDs after incubation with antibody against kinesin-2. Experiments were done in three biological replicates. Error bars are SEM.

Kinesin-1 Is a Major Motor for Lipid Droplets in Hepatocytes. We have earlier reported the motion of purified NLDs and FLDs along in vitro polymerized microtubules (MTs) (18). NLDs moved vigorously over long distance toward MT plus ends, but this motion was reduced significantly for FLDs (motile fraction ~80% for NLDs, ~40% for FLDs). For FLDs, the runs were shorter, and the force exerted by motors against an optical trap was halved (18). Kinesin-1 transports LDs in *Drosophila* embryos, and its knockdown reduces the force against an optical trap (20). Motile fraction, run length, and force of artificial cargos increase with kinesin-1 supplementation (21). Kinesin-1 is also detected on LDs purified from rat liver (22). To test whether kinesin-1 transports LDs in hepatocytes, we investigated LD localization in McA-RH7777 rat hepatoma cells treated with control or kinesin-1–specific siRNA. These spindle-shaped elongated cells had a single microtubule organizing center near the nucleus, with MTs extending along the long axis of the cell in roughly parallel orientation (*SI Appendix*, Fig. S2*B*). Movie S1 shows a LD moving rapidly toward the periphery of a McA-RH7777 cell. Overexpression of MT plus-end tracking protein EB1 in the same cell confirms that this LD is moving to the plus end of MTs (Movie S1). Most LDs were localized at the extreme periphery of cells where the MT plus ends exist, suggesting high activity of kinesin on LDs (Fig. 1*C*, *Upper*; some cells outlined). The peripheral localization was confirmed by measuring the fractional distance of LDs from nucleus (D_F, defiined in Fig. 1*D*). Indeed, another report showed LDs at the periphery of McA-RH7777 cells but the significance of this observation was not discussed (23). Knockdown of kinesin-1 scattered LDs all over McA-RH7777 cells (Fig. 1*C*, *Lower*), as also verified by lower values of D_F (Fig. 1*D*). *SI Appendix*, Fig. S2*C* validates kinesin-1 knockdown in McA-RH7777 cells.

Kinesin-1 knockdown by shRNA also greatly reduced intracellular motion of LDs in human HHL-17 hepatocytes (Movies S2 and S3), as also confirmed by tracking individual LDs (Fig. 1*E*). *SI Appendix*, Fig. S2*D* shows validation of kinesin-1 knockdown in HHL-17 cells. To further confirm that kinesin-1 is present on LDs in cells, we overexpressed Myc-tagged kinesin-1 in HeLa cells. Immunostaining with anti-Myc antibody showed punctate kinesin-1 staining on LDs (*SI Appendix*, Fig. S2*G*). Incubation of NLDs with an antibody against kinesin-1, and also with a recombinant kinesin-1 tail domain peptide (KTD), significantly reduced in vitro LD motion (Fig. 1*F*). A known function blocking antibody K2.4 against kinesin-2 (24) had no effect on LD motility (Fig. 1*G*). Taken together, kinesin-1 is a major motor for transporting LDs in hepatocytes.

Intriguingly, many LDs in liver sections from fed rats were located at the periphery of hepatocytes (Fig. 1*A*; see the red outlined cells). This is also seen in the high value of D_F for these LDs in fed liver (Fig. 1*D*). Early electron micrographs also suggest LD localization toward the periphery of hepatocytes in rat liver (25). We therefore considered it possible that kinesin-1 transports LDs to the periphery of individual hepatocytes inside the liver, more so

CELL BIOLOGY

because MTs emanate from a single focus near the nucleus (presumably the centrosome), and spread out radially with MT plus ends near the hepatocyte cortex (26).

Kinesin-1 Is Recruited to LDs by ARF1 in a Feeding–Fasting-Dependent Manner. We next asked whether kinesin-1 activity on LDs in the liver is a function of the fed/fasted state of the animal. Kinesin-1 could be immunodetected by Western blotting on NLDs and FLDs, with consistently lower intensity on FLDs (Fig. 2*A*). This reduction can explain the earlier report that FLDs move less than NLDs (18). Rat liver lysates showed no feeding–fasting dependence in overall kinesin-1 or cytoplasmic dynein levels (*SI Appendix*, Fig. S3*A*). It is possible that FLD motion is reduced simply because availability of kinesin-1 for LDs becomes limiting when LD numbers increase after fasting. No reduction in kinesin-1 was however observed in liver extract from a fasted rat after LDs had been removed by flotation (*SI Appendix*, Fig. S3*B*), suggesting that kinesin-1 on LDs is negligibly small compared with total soluble kinesin-1 in fasted liver. Thus, reduced in vitro motion of FLDs likely stems from metabolic inhibition of kinesin-1 recruitment to LDs after fasting.

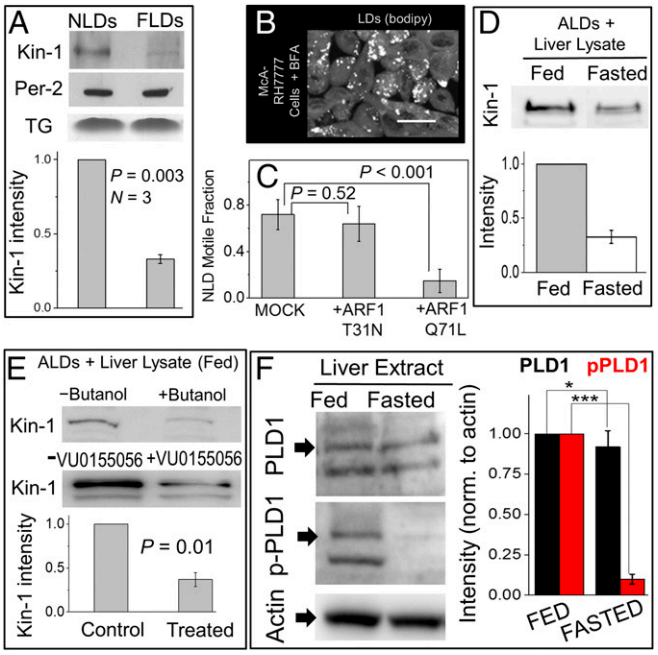

Fig. 2. Kinesin-1 recruitment to LDs depends on feeding–fasting condition, ARF1 and PLD1. (*A*) Western blot for kinesin-1 and perilipin-2 (loading control) on NLDs and FLDs. *Lower* shows band intensity by densitometric analysis. Experiments were done in three biological replicates. Error bars are SEM. (*B*) McA-RH7777 cells treated with Brefeldin-A (BFA). LDs were imaged using BODIPY. (Scale bar, 25 μm.) (*C*) In vitro motile fraction of NLDs in the presence of GST-ARF1-T31N (GDP mimic) and GST-ARF1-Q71L (GTP mimic). Experiments were repeated using LDs from three animals. Error bars are SD. (*D*) Artificial LDs (ALDs) incubated with liver lysate (having the same amount of total protein) from fed and 16-h fasted rats. More kinesin-1 was recruited to ALDs from the fed-rat lysate. (*E*) ALDs incubated with liver lysate from fed rat in presence or absence of phospholipase-D (PLD) inhibitors (1-butanol and VU0155056). Less kinesin-1 was recruited to ALDs in the presence of PLD inhibitors. Fold reduction averaged over different inhibitors is shown. Error bar shows SEM. (*F*) Liver lysate from normally fed or fasted rats was probed with three antibodies: (*i*) against PLD1 to detect total PLD1; (*ii*) phospho-specific antibody against phospho-PLD1 (p-PLD1), which is the active form of PLD1; and (*iii*) actin antibody (for normalization). Normalized band intensity is plotted for fed and fasted samples. Results are averaged over three experiments. Error bar shows SEM. $*P > 0.5$ and $***P < 0.001$. Unpaired *t* test was used for significance (95% confidence).

As discussed earlier, LDs are catabolized efficiently for VLDL production in the fed state (10, 12), and these LDs also move vigorously when extracted from the liver. This could be explained if a molecular factor that promotes LD catabolism also recruits kinesin-1 to LDs. The Ras family GTPase ARF1 recruits effectors to control vesicle budding in the COPI pathway (27). ARF1 is also present on LDs, where it activates lipolysis (5) because ARF1-GTP increases the surface tension of LDs by removing the phospholipid membrane on LDs, thereby generating "reactive" LDs, which exhibit increased fusion with the ER (2, 3). ARF1-GTP is also necessary for lipidation of VLDL, suggesting that these reactive LDs supply TG for VLDL lipidation (28, 29). We therefore suspected that ARF1-GTP recruits kinesin-1 to LDs as a downstream effector, thereby "selecting" reactive LDs to be transported to specific cellular locations (e.g., sER) to supply TG for VLDL production (13, 16). Brefeldin-A (BFA) blocks ARF1 in a GDP-bound state (30), thus inhibiting the binding of downstream effectors (possibly kinesin-1) to ARF1. BFA treatment disrupted the peripheral localization of LDs in McA-RH7777 cells (Fig. 2*B*; compare with Fig. 1*C*, *Upper*) and lowered the value of D_F to 0.38 ± 0.07 (mean ± SEM), similar to kinesin-1 knockdown (Fig. 1*D*). BFA treatment in the presence of nocadozole (to depolymerize MTs) also disrupted the peripheral localization of LDs (*SI Appendix*, Fig. S3*C*). Kinesin-1–driven transport of LDs may therefore require ARF1-GTP. To test this in a purified system, we prepared mutants that mimic the GTP-bound and GDP-bound states of ARF1 (respectively, GST-ARF1-Q71L and GST-ARF1-T31N). These bacterially expressed proteins are not myristoylated (31), and therefore cannot bind the LD membrane (27). If kinesin-1 is recruited to LDs by membrane bound ARF1-GTP, then soluble GST-ARF1-Q71L (GTP mimic) should sequester kinesin-1 away from endogenous ARF1-GTP present on LDs. GST-ARF1-T31N (GDP mimic) should have no effect because it binds neither kinesin-1 nor LDs. Indeed, incubation of NLDs with GST-ARF1-Q71L significantly reduced plus-directed motion, but GST-ARF1-T31N had no effect (Fig. 2*C*). GST-ARF1-Q71L did not affect motion of kinesin-1–coated beads, and therefore did not inhibit enzymatic activity of kinesin-1 (*SI Appendix*, Fig. S3*D*).

A GST pulldown was next performed after mixing GST-ARF1-Q71L or GST-ARF1-T31N with cell lysate from BRL3A hepatocytes. Kinesin-1 was present in a complex with GST-ARF1-Q71L, but not with GST-ARF1-T31N (*SI Appendix*, Fig. S3*E*, *Upper*). Similar results were observed in pulldown using cells coexpressing KIF5B-GFP with ARF1-Q71L-MYC or ARF1-T31N-FLAG (*SI Appendix*, Fig. S3*E*, *Lower*). We do not claim a direct interaction between ARF1 and kinesin-1. Rather, these two are likely part of a larger protein complex resident on the membrane of LDs, whose composition will be a subject of future studies. Similar to kinesin-1, ARF1 amount was higher on NLDs compared with FLDs (*SI Appendix*, Fig. S3*F*). Therefore, more ARF1 is recruited to LDs in the fed state, in turn increasing kinesin-1 on LDs. Enrichment of ARF1 was specific to LDs, because overall ARF1 levels were the same in fed and fasted liver extract (*SI Appendix*, Fig. S3*A*). Higher activity of ARF1 on NLDs was confirmed because the ARF1 effector GGA3 (30) also bound more efficiently to NLDs (*SI Appendix*, Fig. S3*G*). We emphasize that a change in the presence/activity of ARF1 on LDs in the liver of an animal across feeding–fasting cycles, and its downstream metabolic consequences have not been reported before.

Recruitment of Kinesin-1 to LDs Requires PLD1 Activity. How can the feeding–fasting transition control recruitment of ARF1 and kinesin-1 to LDs? Insulin promotes binding of ARF1 to membranes (32, 33). ARF1 activates phospholipase-D1 (PLD1) to convert phophatidylcholine (PC) into phosphatidic acid (PA) on the LD membrane (34). Most importantly, this ARF1-dependent pathway promotes loading of LD-derived TG into VLDL particles (28, 29). However, all of these observations were made in cell culture and have never been connected to the metabolic state of an animal. Combining these reports with the increased presence and activity of ARF1 on NLDs (*SI Appendix*, Fig. S3 *F*

and *G*), we hypothesize that an ARF1-PLD1 dependent pathway is activated on LDs in the fed state (when insulin signaling is active). If this is correct, then more kinesin-1 should get recruited to LDs from cytosol of hepatocytes in the fed state, and this recruitment should require PLD1 activity.

To test this, we prepared protein-free artificial lipid droplets (ALDs) using PC as a phospholipid. ALDs were incubated with liver lysate from fed and fasted rats, separated by flotation, and subjected to Western blotting. These lysates had been centrifuged before the ALD experiment to remove endogenous LDs and were normalized to have equal protein content. Twofold more kinesin-1 was recruited to ALDs from lysates of fed rats, suggesting that the ARF1 pathway is activated in the fed state (Fig. 2*D*). The primary alcohol 1-butanol disrupts PLD1-catalyzed conversion of PC to PA, instead generating phosphatidylbutanol. Addition of 1-butanol blocks events downstream to ARF1-PLD1-PA in an in vitro assay, and this negatively impacts LD formation (35). Kinesin-1 recruitment to ALDs was reduced in the presence of 1-butanol and VU0155056, another inhibitor of PLD (Fig. 2*E*). Significantly more phospho-PLD1 (the active form of PLD1) was detected in crude liver extract from fed rats compared with fasted (Fig. 2*F*), supporting the idea that kinesin-1 is recruited to LDs via ARF1-PLD1, a pathway that is activated by insulin signaling (32–34). This can explain why kinesin-1 recruitment on LDs responds to fed/fasted states.

ARF1 and Kinesin-1 Promote ER–LD Interactions. In hepatocytes, the known lipases that channel LD TG toward VLDL production [e.g., triacylglycerol hydrolase (TGH)] are resident in the ER lumen (7, 36). TGH has a special peptide sequence (HIEL) that targets it to the sER (16), the ER subdomain where VLDL assembly takes place (13). Therefore, sER–LD contacts may facilitate TG mobilization into VLDL in hepatocytes. Interestingly, electron micrographs of rat liver sections suggest that the sER is present at the periphery of hepatocytes (25). Could kinesin-1 promote sER–LD contacts by transporting LDs to the periphery of hepatocytes? Several studies have imaged LD biogenesis at ER–LD contacts (3, 8, 37). However, they use KDEL that does not mark the sER domains (16). In fact, there appears to be no established marker for immunofluorescence staining of sER. In this situation, the direct imaging of sER–LD contacts in hepatocytes, and their dependence on kinesin-1, was not possible here.

As an alternative and possibly more functionally relevant measure of ER–LD contacts, we investigated the LD- and ER-specific localization of proteins that transfer between ER and LDs. Cell death-inducing DFF45-like effector B (Cideb) interacts with ApoB and is present at ER–LD contacts. Cideb is specifically targeted to the sER where VLDL assembly takes place (13). Therefore, Cideb localization on LDs may require kinesin-1 induced ER–LD interactions. Cideb showed intense staining and colocalization with LDs at the periphery of McA-RH7777 cells (Fig. 3 *A* and *C*; yellow arrows in Fig. 3*C*). This suggests that VLDL assembly occurs at these peripheral regions in McA-RH7777 cells. As expected, kinesin-1 knockdown significantly reduced the presence of LDs and Cideb at the peripheral locations (compare Fig. 3*C* with Fig. 3*F*).

FLDs contained less Cideb compared with NLDs (Fig. 3*G*), suggesting that reduced kinesin-1 activity on LDs in the fasted state impairs ER-to-LD transfer of Cideb. To verify this further, we next prepared microsomes and LDs from HHL-17 hepatocytes that had been treated with control and kinesin-1–specific shRNA. Kinesin-1 knockdown increased Cideb on an ER-enriched microsome fraction (*SI Appendix*, Fig. S4*A*). See *SI Appendix*, Fig. S3*H* for ER enrichment on microsomes. Cideb was concomitantly reduced on LDs after kinesin-1 shRNA (*SI Appendix*, Fig. S4*B*). Another protein that transfers from ER to LDs at ER–LD contacts is glycerol-3-phosphate acyltransferase 4 (GPAT4), which catalyzes TG biosynthesis (8). ARF1 knockdown increases GPAT4 on the ER membrane in cell culture assays, possibly because GPAT4 transfer to LDs is blocked (3). Kinesin-1 knockdown also increased GPAT4 in an ER-enriched microsome fraction

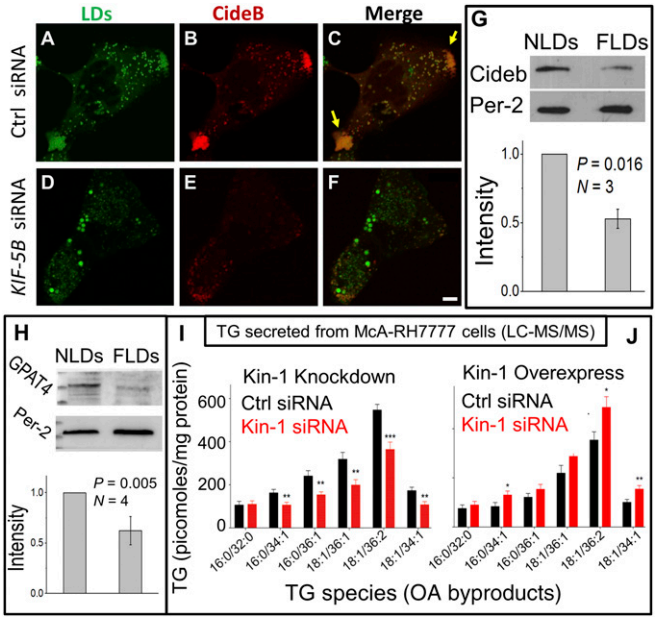

Fig. 3. Kinesin-1–dependent localization of LDs, Cideb recruitment to LDs, and effect on TG secretion from McA-RH7777 cells. (*A–F*) McA-RH7777 hepatoma cells overexpressing Cideb-mcherry were stained with BODIPY to visualize LDs. LDs and Cideb colocalize at the cell periphery in control cells (yellow arrows in *C*). Cideb staining on LDs is reduced after kinesin-1 knockdown. Some larger LDs are observed after kinesin-1 RNAi, likely because lipid mobilization into VLDL is inhibited. (Scale bar, 10 μm.) (*G*) Western blotting of Cideb on NLDs and FLDs. Perilipin-2 is a loading control. Experiments were done in three biological replicates. Error bars are SEM. (*H*) Western blotting shows more GPAT4 on NLDs compared with FLDs. Equal loading was confirmed by perilipin-2 blots. Experiment was repeated on four pairs of fed and fasted animals. Error bars are SEM. The protein marker lane (extreme *Left*) was cut off partially in order to incubate the blot in an antibody solution. (*I*) Secreted levels of TG species following kinesin-1 knockdown from McA-RH7777 cells. Data represent mean ± SEM for six biological replicates. $*P < 0.05$, $**P < 0.01$, $***P < 0.001$. (*J*) Secreted levels of TG species following overexpression of kinesin-myc in McA-RH7777 cells. Data represent mean ± SEM for six biological replicates. $*P < 0.05$, $**P < 0.01$.

(*SI Appendix*, Fig. S4*C*). If kinesin-1 activity is lower on LDs in the fasted state of liver, GPAT4 levels should get reduced on LDs purified from liver. Indeed, FLDs had less GPAT4 than NLDs (Fig. 3*H*). Taken together, these observations suggest that lowered kinesin activity on LDs inhibits ER-to-LD transfer of proteins in a fasted state in the liver.

Kinesin-1 Is Required for TG Loading into VLDL in Cultured Hepatocytes and in Rat Liver. To test whether kinesin-1 controls TG mobilization from LDs into VLDL particles, control and kinesin-1 siRNA-treated McA-RH7777 cells were loaded with oleic acid (OA). Cellular and secreted levels of TG were measured by LC-MS/MS profiling. Kinesin-1 knockdown decreased the amount of OA-derived TG species secreted from cells (Fig. 3*I*) and concomitantly increased their intracellular levels (*SI Appendix*, Fig. S4*D*). TG species targeted by MS, and their MS parameters are presented in *SI Appendix*, Tables S1 and S2. TLC experiments in primary mouse hepatocytes confirmed that kinesin-1 knockdown increases intracellular TG (*SI Appendix*, Figs. S2*E* and S4*E* for RNAi validation). These results indicate that kinesin-1 is not required for FA uptake into hepatocytes, since that should have reduced intracellular TG following kinesin-1 knockdown. It is possible that the availability of lipases and/or sER becomes limiting when LDs accumulate in the liver after fasting. This could also limit catabolism of LD TG and temper TG secretion from the fasted liver. If this is true, overexpressing kinesin-1 should not increase TG secretion from hepatocytes. Contrary to the above conjecture,

CELL BIOLOGY

LC-MS/MS profiling showed significantly more TG secreted into medium from kinesin-1 overexpressing cells compared with control (Fig. 3*J* and *SI Appendix*, Fig. S4*F* for kinesin-1 expression).

Next, we knocked down kinesin-1 in rat liver using shRNA plasmid against *KIF-5B* complexed with a polyethylenimine (PEI)-based transfection reagent. To minimize unknown effects of kinesin-1 knockdown in the animal, shRNA-PEI dosage was optimized to achieve only partial knockdown of kinesin-1 (~40% reduction observed, see *SI Appendix*, Fig. S4*G*). Tyloxapol was used to block VLDL catabolism and clearance (13). Glycerol phosphate oxidase (GPO) assays showed significant reduction in serum TG in shRNA-PEI–treated animals (Fig. 4*A*). Accordingly, serum from shRNA-treated animals was more transparent (Fig. 4*A*, *Inset*). TG reduction in serum after kinesin-1 shRNA was also confirmed by TLC (*SI Appendix*, Fig. S4*H*). Considering only partial (~40%) kinesin-1 knockdown, the 30% reduction in serum TG suggests a significant role for kinesin-1 in supplying TG to VLDL particles. To further verify this, we prepared serum from control and kinesin-1 shRNA-treated rats. Serum was subjected to density gradient ultracentrifugation, ApoB was immunoprecipitated and assessed by Western blotting with antibody against ApoB. ApoB shifted to higher density fractions in kinesin-1 shRNA-treated rats, suggesting that the secreted lipoprotein particles are TG deficient (*SI Appendix*, Fig. S5*A*). ApoB inside and secreted from hepatocytes did not change after kinesin-1 knockdown (*SI Appendix*, Fig. S5 *B* and *C*). Taken together, kinesin-1 is specifically required to supply TG during VLDL maturation, and absence of kinesin-1 results in secretion of TG-deficient VLDL particles.

ApoB amount in rat liver extract (*SI Appendix*, Fig. S5*D*) and rat serum (*SI Appendix*, Fig. S5*E*) was unchanged between fed and fasted states. ER-resident lipases mobilize LD TG for VLDL production (7, 36). An LC-MS based TG substrate hydrolysis assay was used to measure lipase activity in ER-enriched microsome membranes. Microsomes prepared from fed and fasted rats showed no difference in TG hydrolysis activity (*SI Appendix*, Fig. S6*A*). Therefore, TG secretion across fed/fasted states is not controlled by ApoB availability or lipase activity.

Kinesin-1 Knockdown Inhibits Hepatitis-C Replication and Secretion. HCV is secreted as a lipoviral particle from hepatocytes. ARF1 inhibition (38) or Cideb knockdown inhibits HCV replication, and Cideb interacts with a viral protein NS5A in the sER of hepatocytes (39). HCV replication requires that virus-encoded proteins physically transfer from the ER to LDs in hepatocytes (17), and it is possible that ARF1 and kinesin-1 facilitate such ER–LD contacts. To test this, Huh7.5 cells were subjected to control or kinesin-1–specific shRNA (*SI Appendix*, Fig. S2*F* for RNAi verification). Cells were then transfected with HCV-RNA, and total RNA was isolated from cells and cell culture supernatant. HCV genomic RNA was estimated using qRT-PCR (40). Kinesin-1 knockdown decreased positive and negative sense HCV-RNA inside cells (Fig. 4*B*) and secreted into culture medium (Fig. 4*C*). The HCV capsid protein "core" was detected on LDs in control cells, but was reduced after kinesin-1 knockdown (*SI Appendix*, Fig. S6*B*). Western blotting showed that intracellular core was reduced significantly after kinesin-1 knockdown (*SI Appendix*, Fig. S6 *C* and *D*). Kinesin-1 knockdown therefore inhibits HCV replication, which expectedly reduces the total HCV core in cells.

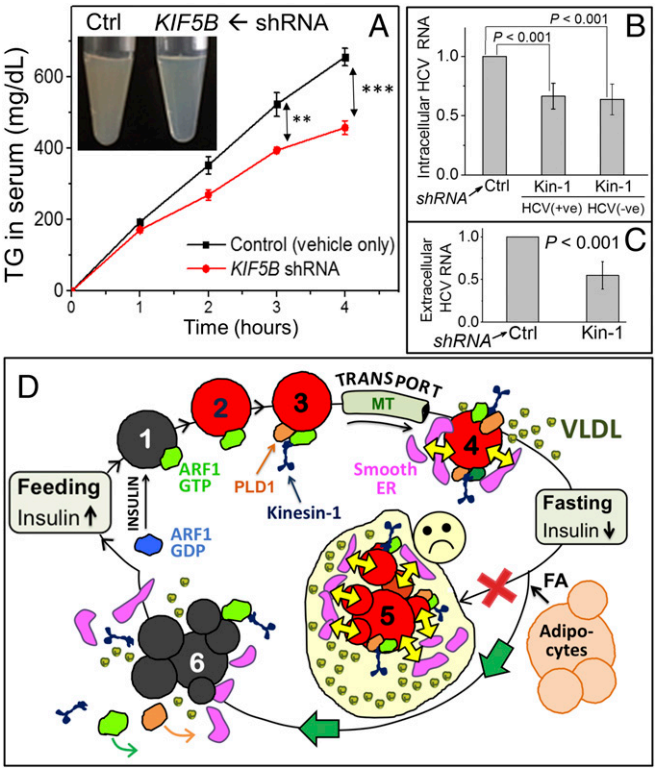

Fig. 4. Kinesin-1 is required for VLDL lipidation and HCV replication. (*A*) Serum TG in rats treated with only PEI transfection reagent (control) or *KIF-5B* shRNA + PEI. Serum TG was quantified using a GPO colorimetric method. Experiments were done in three biological replicates. Error bars are SEM. $^{**}P = 0.02$, $^{***}P = 0.003$. (*Inset*) Serum from control (turbid) and kinesin-1 knockdown rats (transparent) 4 h after tyloxapol injection. (*B*) Change in intracellular positive- and negative-sense HCV-RNA estimated by qRT-PCR. Relative amounts are plotted after normalization with an internal control GAPDH (glyceraldehyde 3-phosphate dehydrogenase) RNA. Measurement at 48 h posttransfection. (*C*) Change in extracellular (secreted) HCV-RNA estimated by qRT-PCR. Relative amounts are plotted after normalization with GAPDH RNA. Cell culture medium was collected at 72 h posttransfection. (*D*) Hypothesis for control of VLDL-triglyceride secretion from liver across feeding–fasting cycles. (Fed) A small pool of LDs is efficiently mobilized toward VLDL lipidation in the fed state. (state 1) Insulin activates ARF1, resulting in binding of ARF1-GTP to LDs. (state 2) ARF1-GTP removes phospholipids to make the LD reactive (red color). (state 3) ARF1-GTP also recruits kinesin-1 to the reactive LD in a complex with other proteins (e.g., PLD1). Kinesin-1 transports LDs along MTs to hepatocyte periphery. (state 4) This results in physical interactions between LDs and smooth ER. Lipases and phospholipids are exchanged efficiently (large yellow arrows), facilitating efficient TG mobilization from LDs for VLDL lipidation and secretion. (Fasting) FA released from adipose tissue is esterified and stored as LDs to massively increase LD TG in hepatocytes. If this large LD pool remained reactive (red) and maintained contacts with the smooth ER (shown in state 5), then VLDL serum TG would increase dangerously (sad face). To avoid this, an alternate pathway is activated (green arrows): Fasting-induced reduction in insulin inactivates ARF1, causing ARF1 and kinesin-1 to dissociate from LDs (state 6). These LDs are less reactive (gray) and interact less with the peripheral smooth ER. This ensures that TG secretion from fasted liver (state 6) continues at approximately the same rate as fed (state 4), while still permitting the fasted liver to store large amounts of TG.

Discussion

A small pool of LDs is constantly and efficiently catabolized in hepatocytes to produce VLDL (10, 12, 15). The site of this catabolism is likely the sER, because the relevant lipase (TGH) is resident on the sER in hepatocytes (16). This is reasonable, because VLDL is assembled at the sER (13). Because sER and TGH are both found at the periphery of hepatocytes (16), and because kinesin transports LDs to MT plus ends (9, 20), we propose a model whereby kinesin-1–driven motion of LDs engineers sER–LD interactions (Fig. 4*D*). Our work reveals a molecular pathway involving insulin signaling, ARF1 and kinesin that makes LDs reactive, due to the presence of active ARF1-GTP, and also "selects" them for transport to the sER and for inducing LD–sER contacts. The sER-resident lipases (e.g., TGH) likely access the TG in LDs via such contacts. The lipolytic products could be reesterified and secreted into the ER lumen as VLDL precursors (15).

We further provide evidence for how ER–LD interactions are inhibited after fasting to prevent oversecretion of TG

from the liver. Lowered insulin likely reduces PLD1 activity and displaces ARF1 and kinesin from LDs to down-regulate ER–LD contacts, thus tempering TG secretion after fasting (Fig. 4*D*). Glucose starvation distributes LDs peripherally in a kinesin-2–dependent manner along detyrosinated MTs in cultured fibroblasts, facilitating LD–mitochondria interactions and fatty acid oxidation (9). Therefore, different kinesins may channel LD TG toward VLDL assembly (as shown here) or fatty acid oxidation in a starved state. Our model potentially explains how plasma-TG levels are maintained homeostatically, even after massive TG accumulation in the fasted liver. Lipid may also be added to VLDL in the Golgi (41), but considering the peripheral location of Cideb and sER, it appears that the kinesin-1–dependent pathway specifically facilitates TG delivery for VLDL assembly in the sER. We believe that this kinesin pathway supplies lipid for assembly of the more buoyant TG-rich form of VLDL (VLDL1), because we found kinesin-1 knockdown to result in secretion of poorly lipidated VLDL particles of higher density. Kinesin-1 knockdown also reduced intracellular and secreted HCV-RNA. HCV viral proteins must transfer from the ER of infected hepatocytes to LDs (17). Such transfer would require ER–LD contacts, which are likely diminished when kinesin-1 activity on LDs is low. HCV replication and assembly is much debated (17). The kinesin-1–dependent mechanism elucidated here to facilitate ER–LD interactions may help understand fundamental aspects of HCV pathobiology.

Materials and Methods

See *SI Appendix* for detailed information. Reagents were purchased from Sigma-Aldrich unless otherwise mentioned. All animal protocols were approved by the Institutional Animal Ethics Committee (IAEC) formulated by the Committee for the Purpose of Control and Supervision of Experiments on Animals (CPCSEA), India. For reagents, plasmids, cell culture, and animal procedures, see *SI Appendix*, Sections 1–3. LDs were prepared from rat liver by sucrose density gradient (*SI Appendix*, Sections 5 and 8) and assayed for in vitro motility (*SI Appendix*, Section 6). ALDs prepared using glyceryl trioleate and PC were incubated with liver lysate before centrifugation and Western blotting (*SI Appendix*, Section 15). Cells infected with adenoviral shRNA were separated into LDs and soluble and membrane fractions (*SI Appendix*, Section 16). Rats were injected with kinesin-1 shRNA plasmid complexed with jetPEI, and later with Triton WR-1339. Serum was prepared for TG estimation and fractionation of ApoB containing lipoproteins (*SI Appendix*, Sections 17 and 23). Cellular and secreted TG was measured by LC-MS (*SI Appendix*, Section 21). ApoB was measured in cells and in liver lysates by Western blotting after immunoprecipitation (*SI Appendix*, Section 22). Liver lysate was subjected to ultracentrifugation to prepare microsomes and the membrane proteins were isolated for substrate hydrolysis assay (*SI Appendix*, Sections 24 and 25). Huh7.5 cells were infected with adenoviral shRNA followed by transfection with HCV-JFH-1 RNA. Cells and media were used for RNA isolation and qRT-PCR (*SI Appendix*, Section 26). See details of statistical analysis in *SI Appendix*, Section 27.

ACKNOWLEDGMENTS. We thank K. Sadh, J. Singh, N. Mehendale, D. Kelkar, S. Thakur, and S. Ojha for help with experiments; R. Lehner, J. Varghese, D. Brasaemle, J. Lippincott-Schwartz, and A. Chattopadhyay for discussions; V. Malhotra, N. Balasubramanian, A. H. Patel, A. Akhmanova, and K. Verhey for reagents; J. Kalia for access to the LC-MS facility; and Dr. Suryavanshi and the Tata Institute of Fundamental Research Animal House for maintaining and providing animals for experiments. Funding was provided by the Department of Atomic Energy (Government of India) and the Wellcome Trust–Department of Biotechnology India Alliance (Grants IA/S/11/2500255 to R.M., IA/I/15/2/502058 to S.S.K., and IA/E/11/1/500417 to P.R.) and Indian Institute of Science Education and Research Pune (S.S.K.). S.D. acknowledges the Jagadish Chandra Bose fellowship. G.S. was supported by a Council of Scientific and Industrial Research fellowship.

1. Ruggles KV, Turkish A, Sturley SL (2013) Making, baking, and breaking: The synthesis, storage, and hydrolysis of neutral lipids. *Annu Rev Nutr* 33:413–451.
2. Thiam AR, et al. (2013) COPI buds 60-nm lipid droplets from reconstituted water-phospholipid-triacylglyceride interfaces, suggesting a tension clamp function. *Proc Natl Acad Sci USA* 110:13244–13249.
3. Wilfling F, et al. (2014) Arf1/COPI machinery acts directly on lipid droplets and enables their connection to the ER for protein targeting. *Elife* 3:e01607.
4. Beller M, Thiel K, Thul PJ, Jäckle H (2010) Lipid droplets: A dynamic organelle moves into focus. *FEBS Lett* 584:2176–2182.
5. Beller M, et al. (2008) COPI complex is a regulator of lipid homeostasis. *PLoS Biol* 6:e292.
6. Cohen JC, Horton JD, Hobbs HH (2011) Human fatty liver disease: Old questions and new insights. *Science* 332:1519–1523.
7. Wang H, et al. (2010) Altered lipid droplet dynamics in hepatocytes lacking triacylglycerol hydrolase expression. *Mol Biol Cell* 21:1991–2000.
8. Wilfling F, et al. (2013) Triacylglycerol synthesis enzymes mediate lipid droplet growth by relocalizing from the ER to lipid droplets. *Dev Cell* 24:384–399.
9. Herms A, et al. (2015) AMPK activation promotes lipid droplet dispersion on detyrosinated microtubules to increase mitochondrial fatty acid oxidation. *Nat Commun* 6:7176.
10. Wiggins D, Gibbons GF (1992) The lipolysis/esterification cycle of hepatic triacylglycerol. Its role in the secretion of very-low-density lipoprotein and its response to hormones and sulphonylureas. *Biochem J* 284:457–462.
11. Yang LY, Kuksis A, Myher JJ, Steiner G (1996) Contribution of de novo fatty acid synthesis to very low density lipoprotein triacylglycerols: Evidence from mass isotopomer distribution analysis of fatty acids synthesized from [2H6]ethanol. *J Lipid Res* 37:262–274.
12. Gibbons GF, Wiggins D (1995) Intracellular triacylglycerol lipase: Its role in the assembly of hepatic very-low-density lipoprotein (VLDL). *Adv Enzyme Regul* 35:179–198.
13. Ye J, et al. (2009) Cideb, an ER- and lipid droplet-associated protein, mediates VLDL lipidation and maturation by interacting with apolipoprotein B. *Cell Metab* 9:177–190.
14. Takahashi K, et al. (2010) Glucagon regulates intracellular distribution of adipose differentiation-related protein during triacylglycerol accumulation in the liver. *J Lipid Res* 51:2571–2580.
15. Gibbons GF, Islam K, Pease RJ (2000) Mobilisation of triacylglycerol stores. *Biochim Biophys Acta* 1483:37–57.
16. Gilham D, Alam M, Gao W, Vance DE, Lehner R (2005) Triacylglycerol hydrolase is localized to the endoplasmic reticulum by an unusual retrieval sequence where it participates in VLDL assembly without utilizing VLDL lipids as substrates. *Mol Biol Cell* 16:984–996.
17. Filipe A, McLauchlan J (2015) Hepatitis C virus and lipid droplets: Finding a niche. *Trends Mol Med* 21:34–42.
18. Barak P, Rai A, Rai P, Mallik R (2013) Quantitative optical trapping on single organelles in cell extract. *Nat Methods* 10:68–70.
19. Barak P, Rai A, Dubey AK, Rai P, Mallik R (2014) Reconstitution of microtubule-dependent organelle transport. *Methods Enzymol* 540:231–248.
20. Shubeita GT, et al. (2008) Consequences of motor copy number on the intracellular transport of kinesin-1-driven lipid droplets. *Cell* 135:1098–1107.
21. Vershinin M, Carter BC, Razafsky DS, King SJ, Gross SP (2007) Multiple-motor based transport and its regulation by Tau. *Proc Natl Acad Sci USA* 104:87–92.
22. Turró S, et al. (2006) Identification and characterization of associated with lipid droplet protein 1: A novel membrane-associated protein that resides on hepatic lipid droplets. *Traffic* 7:1254–1269.
23. Gannon J, et al. (2014) ARFGAP1 is dynamically associated with lipid droplets in hepatocytes. *PLoS One* 9:e111309.
24. Morris RL, Scholey JM (1997) Heterotrimeric kinesin-II is required for the assembly of motile 9+2 ciliary axonemes on sea urchin embryos. *J Cell Biol* 138:1009–1022.
25. Palade GE, Siekevitz P (1956) Liver microsomes; an integrated morphological and biochemical study. *J Biophys Biochem Cytol* 2:171–200.
26. Novikoff PM, et al. (1996) Three-dimensional organization of rat hepatocyte cytoskeleton: Relation to the asialoglycoprotein endocytosis pathway. *J Cell Sci* 109:21–32.
27. Donaldson JG, Jackson CL (2011) ARF family G proteins and their regulators: Roles in membrane transport, development and disease. *Nat Rev Mol Cell Biol* 12:362–375.
28. Asp L, et al. (2005) Role of ADP ribosylation factor 1 in the assembly and secretion of ApoB-100-containing lipoproteins. *Arterioscler Thromb Vasc Biol* 25:566–570.
29. Asp L, Claesson C, Boren J, Olofsson SO (2000) ADP-ribosylation factor 1 and its activation of phospholipase D are important for the assembly of very low density lipoproteins. *J Biol Chem* 275:26285–26292.
30. Niu TK, Pfeifer AC, Lippincott-Schwartz J, Jackson CL (2005) Dynamics of GBF1, a Brefeldin A-sensitive arf1 exchange factor at the golgi. *Mol Biol Cell* 16:1213–1222.
31. Ha VL, Thomas GMH, Stauffer S, Randazzo PA (2005) Preparation of myristoylated Arf1 and Arf6. *Methods Enzymol* 404:164–174.
32. Shome K, Vasudevan C, Romero G (1997) ARF proteins mediate insulin-dependent activation of phospholipase D. *Curr Biol* 7:387–396.
33. Li H-S, et al. (2003) The guanine nucleotide exchange factor ARNO mediates the activation of ARF and phospholipase D by insulin. *BMC Cell Biol* 4:13.
34. Nakamura N, Banno Y, Tamiya-Koizumi K (2005) Arf1-dependent PLD1 is localized to oleic acid-induced lipid droplets in NIH3T3 cells. *Biochem Biophys Res Commun* 335:117–123.
35. Marchesan D, et al. (2003) A phospholipase D-dependent process forms lipid droplets containing caveolin, adipocyte differentiation-related protein, and vimentin in a cell-free system. *J Biol Chem* 278:27293–27300.
36. Lehner R, Lian J, Quiroga AD (2012) Lumenal lipid metabolism: Implications for lipoprotein assembly. *Arterioscler Thromb Vasc Biol* 32:1087–1093.
37. Salo VT, et al. (2016) Seipin regulates ER-lipid droplet contacts and cargo delivery. *EMBO J* 35:2699–2716.
38. Matto M, et al. (2011) Role for ADP ribosylation factor 1 in the regulation of hepatitis C virus replication. *J Virol* 85:946–956.
39. Cai H, et al. (2016) Cell-death-inducing DFFA-like effector B contributes to the assembly of hepatitis C virus (HCV) particles and interacts with HCV NS5A. *Sci Rep* 6:27778.
40. Li Q, et al. (2016) Hepatitis C virus depends on E-cadherin as an entry factor and regulates its expression in epithelial-to-mesenchymal transition. *Proc Natl Acad Sci USA* 113:7620–7625.
41. Li X, et al. (2012) Opposing roles of cell death-inducing DFF45-like effector B and perilipin 2 in controlling hepatic VLDL lipidation. *J Lipid Res* 53:1877–1889.